scientific reports

Check for updates

OPEN

Investigation of FF-MAS oxysterole's role in follicular development and its relation to hedgehog signal pathway

Selim Zırh[1,4], Elham Bahador Zırh[2,4], Süleyman Erol[3,4], Lale Karakoç Sökmensüer[4], Gürkan Bozdağ[5] & Sevda Fatma Müftüoğlu[4✉]

The Hedgehog signaling pathway plays a crucial role in folliculogenesis; however, the association between FF-MAS oxysterol activity in folliculogenesis and the Hedgehog signaling pathway has not been revealed. The evaluation of FF-MAS activity in polycystic ovary syndrome (PCOS) with folliculogenesis disorder might provide a new approach to tackle follicular and oocyte maturation failure. The question is: does FF-MAS oxysterol affect granulosa cell (GC) proliferation? If so, is this effect facilitated through the Hedgehog pathway? To answer these questions, GCs were isolated from follicle fluids obtained from patients undergoing oocyte retrieval during in vitro fertilization (IVF) treatment. After the isolated GCs were incubated in different cell culture media, the levels of Hedgehog pathway components (SMO, Gli1) were measured by using immunohistochemical methods, cytoELISA, and qRT-PCR. Meanwhile, cell proliferation rates were determined. Significant increases ($p < 0.001$) in SMO and Gli1 expressions and cell proliferation were observed in the FF-MAS-treated subgroups of both PCOS and male factor participants compared to the FF-MAS deficient subgroup. Remarkably, FF-MAS positively affected the pathway components despite the pathway inhibitor cyclopamine. Although the increase in Hedgehog pathway components was slightly higher in the male factor group (MF), it was not statistically significant. In our study, we demonstrated for the first time the molecular effect of FF-MAS on human GCs in folliculogenesis. Since FF-MAS is already used in assisted reproductive techniques in animals and is known to be synthesized in the human body, it could be considered a new approach in human IVF treatments.

Keywords FF-MAS, Follicle development, Granulosa cells, Oxysterols, PCOS, Steroidogenesis

Polycystic ovary syndrome (PCOS) is characterized by both clinical and biochemical hyperandrogenemia, oligomenorrhea, or amenorrhea, along with at least 18 ovarian cysts as detected by ultrasound examination. The disease, which has a 5–10% incidence rate among women of reproductive age, serves as a principal cause of ovary-related infertility[1]. While numerous metabolic, hormonal, and structural effects are present in the pathophysiology of PCOS, and many clinical and preclinical studies have been conducted on the syndrome, the complete pathology of the disease remains largely undisclosed[2]. Patients with PCOS are often observed to have a significant amount of cystic follicles, the diameter of which can grow to between 2 and 9 mm. These follicles often feature a broad antrum, which is bordered by only one or two layers of granulosa cells, indicating a pathology in granulosa cell proliferation and organization. Granulosa cells play a significant role in the structure and function of the female gamete, by enveloping oocyte. These cells control the molecular passage to the oocyte through the basal lamina and produce follicular fluid. Under hormonal control, granulosa cells generate factors to maintain the oocyte meiosis process. These functions make granulosa cells essential to ensuring fertility[3,4].

Active SHH signaling targets (PTCH, SMO, and Gli1) have been identified in the granulosa cells and cumulus oophorus of rodents[5], felines[6], and pigs[7]. It has been shown in Gli1 (+) human granulosa cells, that the

[1]Faculty of Medicine, Department of Histology and Embryology, Erzincan Binali Yıldırım University, Erzincan, Turkey. [2]Faculty of Medicine, Department of Histology and Embryology, TOBB Economy and Technology University, Ankara, Turkey. [3]Ankara Etlik Lady Zübeyde Gynaecology Education and Research Hospital, Assisted Reproductive Techniques, Ankara, Turkey. [4]Faculty of Medicine, Department of Histology and Embryology, Hacettepe University, Ankara, Turkey. [5]Faculty of Medicine, Obstetrics and Gynecology, Koç University, Ankara, Turkey. ✉email: smuftuog@hacettepe.edu.tr

inhibition of Dhh and Ihh prevents folliculogenesis and the development of theca cells[8]. In the context of in vitro maturation experiments, Ptch1 protein expression has been observed following the addition of Shh protein to the culture medium, and discussions have been held regarding the pathway's effect on embryonic development with oocyte maturation[7–9].

The Hedgehog cell signaling pathway plays a crucial role in adult stem cell renewal processes, as well as in the embryological development of gonads. Defects in this pathway can lead to gonadal dysgenesis (DHh)[10].

In the canonical Hh pathway, Hedgehog ligand proteins bind to the negative regulatory transmembrane protein patched (Ptch), resulting in Ptch inhibition. This eliminates Ptch's inhibition on Smoothened (SMO). When activated, SMO triggers a downstream signaling cascade, causing the translocation of Glioma-associated (Gli) family proteins. These Gli proteins are the end products of the pathway and are a type of zinc finger transcription factor. Once translocated to the nucleus, active Gli transcription factors either activate or inhibit target gene expression[10]. The Hedgehog signaling pathway encompasses two types of non-canonical pathways. In the first type, independently of SMO and Gli, Ptch1 binds and inhibits Cyclin B1 in the absence of a ligand. This inhibition of Cyclin B1 prompts apoptosis. When Ptch1 is suppressed by a ligand, Cyclin B1 is released, enabling cell proliferation. In the second type, SMO binds to the Gi protein, independent of Ptch and Gli, leading to aerobic glycolysis, glucose intake, and a $Ca+$ release from the smooth endoplasmic reticulum[11].

Cyclopamine, an Hh pathway inhibitor, operates by binding to SMO, which prevents the production of the pathway's end products. Numerous studies have explored the use of cyclopamine in chemotherapy by its antiproliferative effect[12].

Oxysterols are oxidized cholesterols that are produced as intermediate steps in steroid synthesis. Despite being unstable molecules with a short half-life, they play a key role in both the steroid synthesis pathway and in biological systems due to the tasks they fulfill in molecular cell pathways[13]. Furthermore, oxysterols are crucial for the Hh pathway, affecting the posttranslational modification of ligands, and there is an oxysterol binding site in the extracellular part of the SMO protein[13,14]. In their publication in 1998, Byskov et al. isolated a previously undetected oxysterol from the follicular fluid of human Graafian follicles and named it follicular fluid-meiosis activator sterol (FF-MAS) (4,4-dimethyl-5α-cholesterol-8,14,24-triene-3β-ol)[15,16]. Cumulus cells produce FF-MAS in GOCs stimulated with FSH in vitro, and FF-MAS enables the oocyte to continue meiosis[17]. It is involved in the transition to metaphase 2 in mouse oocyte maturation in vitro and in the progression from 2-cell blastomere to blastocyst[15,18]. In a recent study conducted in pig oocytes, it was observed that MAPK pathway components increased in groups with increased FF-MAS using crystallins that inhibit and stimulate FF-MAS formation[19]. However, there is not enough information in the literature about which cellular pathway FF-MAS exerts this effect on human oocytes.

It is known that the Hedgehog pathway plays a role in ovarian follicle development and increases granulosa cell proliferation[20]. Granulosa cell proliferation is impaired and insufficient in PCOS[21]. Based on these two parts of information, we can assume that the Hedgehog pathway will increase proliferation in PCOS. In our study, proliferation decreased in the group administered cyclopamine (Hedgehog pathway inhibitor), while the increase was correlated with proliferation rates in the groups in which the components of the pathway increased. In addition, since there is an oxysterol binding site in the extracellular part of the SMO protein, which is a component of the Hedgehog pathway, the pathway's relationship with oxysterols is also known[22,23]. We planned our study by hypothesizing that the effect of FF-MAS on follicle development may be effective based on the components of Hh pathway.

The goal of this study is to illuminate the potential relationship between the FF-MAS oxysterol and the Hh signaling pathway, which stimulates the proliferation of granulosa cells and aids in oocyte maturation. For this purpose, follicular fluids from PCOS patients with cell proliferation disorders and healthy women, who underwent IVF treatment due to male infertility as a control group, were collected. Primary granulosa cell cultures were then derived from these follicular fluids. Within these main groups and the normal human granulosa cell line, we examined SMO and Gli1 expressions among FF-MAS-supplemented and non-supplemented subgroups.

Materials and methods
Participants and study design
The granulosa cells of 16 women who applied to the Hacettepe University ART Clinic between June 2018 and July 2020 were isolated and included in this study. Eight of these women, who sought treatment due to male infertility, were designated as the control group. The other eight are patients with PCOS, who present with multiple cystic follicles, high androgen hormone levels, and insulin resistance. However, these patients did not have any cysts during in vitro fertilization, and follicular development was observed. Additionally, the immortalized human granulosa cell line, HGL5 (catalog number T0650, abm, Canada), was used as a standard control. Participants with any other systemic diseases were not included in the study. The entire process was explained to the participants and informed consents were obtained.

Cell isolation and culturing, cell proliferation assesment
Incoming follicle fluids were diluted 1:1 with dPBS. This solution was poured onto the separation solution (Lypmphosep, Biowest, France) and centrifuged at +4 °C at 2500 rpm (600 g) for 30 min. The buffy coat, which floated between the two formed phases, was collected and mixed 1:1 with the basal Dulbecco's Modified Eagle's Medium-F12 (DMEM-F12, Capricorn Scientific, Germany) medium. This mixture was then centrifuged at 260 g for 5 min. The resulting pellet was seeded into culture flasks with DMEM-F12 (5% fetal bovine serum [FBS, Capricorn Scientific, Germany], 4% L-glutamine [Capricorn Scientific, Germany], 1% penicillin-streptomycin-amphotericin B [Biowest, France]) and Bio-Amf 1 medium (Biological Industries, USA) in a 1:1 ratio. For subsequent feeds, only the complete DMEM-F12 medium was used. All participant samples were cultured until the 4th passage and included in the experiments[24]. Cell proliferation was assessed at dosages of 0, 0.1, 10, and

100 μM FF-MAS with WST-1 (Roche, Switzerland) at the 0, 24, and 48 h timepoints and the doubling time was calculated.

Experimental groups

Each participant's sample and the HGL5 cells were divided into four subgroups. These are 1 (F): the FF-MAS subgroup; 2 (F + Cyc): the FF-MAS plus cyclopamine subgroup; 3 (Cyc): the cyclopamine subgroup; and 4 (CG): the Control subgroup. To examine the relationship between FF-MAS and Hh signaling pathway, cyclopamine, a canonical inhibitor of the Hh pathway, was added to the experimental groups. Thus, we examined whether FF-MAS proceeds via the canonical pathway of the Hh signaling pathway.

Samples of the subgroup F received a complete medium containing 10 μM FF-MAS (Avanti Polar Lipids, USA), which is the ED50 value, were obtained as a result of the WST-1 (Roche, Switzerland) experiment in both participant groups and the HGL5 cells. In the Cyc subgroup, the medium contains only previously specified 10 μM cyclopamine[25,26]. The F + Cyc group received a medium containing 10 μM FF-MAS and 10 μM cyclopamine (Sigma Aldrich, USA). The CG group received only a medium containing only solvents of FF-MAS (Absolute ethanol: 1 μl/100 μl) and cyclopamine (DMSO: 0.082 μl/100 μl).

ELISA measurement

Initially, 1×10^4 cells were seeded onto 96-well plates, with six wells allocated per subgroup. After a 24-h incubation period, a cell proliferation assessment was performed, following which an appropriate medium was added to the subgroups and further incubated for 48 h. The medium was then removed, and the cells were washed with PBS for 5 min and subsequently fixed with 0.05% glutaraldehyde at room temperature for 10 min. After a further round of washing with PBS, primary antibodies [Anti-SMO rabbit anti-human polyclonal antibody (bs-2801R, Bioss, USA; 1/200) and Anti-Gli1 rabbit anti-human polyclonal antibody (bs-1206R, Bioss, USA; 1/200)] and a secondary antibody [Peroxidase AffiniPure Goat Anti-Rabbit IgG (H + L; 111-035-003, Jackson ImmunoResearch, USA; 1: 1000)] were applied. Following a 5-min wash with PBS, the cells were incubated with chromogen diaminobenzidine (DAB 11718096001, Roche, Switzerland) for 20 min on a shaker and kept in darkness at room temperature. Subsequently, optical density measurements were conducted using an ELISA reader (Versamax microplate reader) at a wavelength between 490 and 650 nm. The data was evaluated using Softmax Pro5 software.

Immunoperoxidase (IP) and immunofluorescent (IF) labeling

Primary cultures and HGL5 cell line cells were seeded onto two 8-well slides at a density of 1×10^4 cells/well and allowed to attach for 24 h. Following this period, the cells were rinsed with PBS and fixed with 100% methanol at room temperature for 5 min. The cells were then washed three times, each for 5 min with PBS. Notably, only for Gli1 which is expressed in the nucleus, it was necessary to perform permeabilization with 0.1% Tween20 (P1379, Sigma Aldrich, USA) before proceeding to wash the cells. After applying peroxide and blocking with serum, the cells were exposed to the primary antibodies, Anti-SMO antibody (1/200) and Anti-Gli1 antibody (1/200). The cells were then incubated with the appropriate secondary antibody (Peroxidase AffiniPure Goat Anti-Rabbit IgG 111-035-003, Jackson ImmunoResearch, USA, 1: 1000; Alexa Fluor® 488-AffiniPure Goat Anti-Rabbit IgG 111-545-003, Jackson ImmunoResearch, USA, 1:1000) at room temperature for 1 h. Following another wash, DAB and Mayer's hematoxylin were employed for IP and nuclear labeling respectively. For IF, DAPI was used in the labeling of the nucleus.

IP and IF labeled cells were imaged using a light microscope equipped with a camera (Leica DM6B + Leica DFC7000T camera, Wetzlar, Germany) and imaging software (LAS X, Leica, Wetzlar, Germany). The same system's fluorescent attachment was also utilized for imaging IF labels.

To evaluate the labelings, micrographs were captured using the Leica DFC7000T camera and the LAS X program, specifically in five to seven randomly chosen areas at 40× magnification. The immunoreactivity in IP-labeled cells was semi-quantitatively evaluated by the H-score[27]. This procedure involved evaluating the intensity of labeling with primary antibodies, where 0 corresponds to no staining, 1 to weak staining, 2 to notable staining, and 3 to strong, intense staining. Also, the percentage of labeled cells, ranging from 0 to 100%, was assessed. The evaluations were conducted by two researchers, and the average score received from the two was used.

Intensity measurements were carried out using ImageJ (V. 1.53a, NIH, USA) on the micrographs to evaluate immunofluorescence markings[28]. Images were analyzed using a software program (Image J packaged with 64-bit Java 1.8.0_172, NIH, USA) by selecting one cell at a time in an image and measuring area, average gray value, and integrated intensity. "The fluorescence intensity was calculated according to the following formula: corrected total cell fluorescence (CTCF) = integrated intensity − (mean fluorescence of background readings × area of the selected cell).

qRT-PCR

Total RNAs from placental tissues were extracted using the NucleoZol reagent (Macherey-Nagel, Germany), following the manufacturer's protocol. RNA samples were reversed-transcribed into cDNA using the OneScript® Plus cDNA Synthesis Kit (ABM, Canada). Real-time PCR analysis of Smoothened, Frizzled class receptor (SMO), GLI family zinc finger 1 (GLI1) mRNA was performed using the BrightGreen 2× qPCR MasterMix-No Dye (ABM, Canada) and the LightCycler 480 Real-time PCR system (Roche, Switzerland). Each sample was run in duplicate with the amplification conditions set as follows: 95 °C for 5 min to activate the Taq DNA polymerase, followed by 40 cycles of 95 °C for 10 s and 55 °C for 30 s, and then the Melting Curve set at 95 °C for 5 s and 65 °C for 1 min, maintained at 97 °C continuously for the PCR. The resulting gene expression profile was measured using the ACTB housekeeping gene. The Threshold cycles (Ct) for each reaction were calculated and used to quantify the amount of starting template in the reaction. The proportions of the genes of interest in a sample

were represented as the Ct value differences (ΔCt) between the respective gene and the ACTB. The relative gene expression among samples was calculated using the 2-ΔΔCT method[29] as described elsewhere. The primers used in our study were as follows: SMO (Forward): CAAGATCAACGAGACCAT, (Reverse): CCTGACATAGCACA TAGT; GLI1 (Forward): AGTACATGCTGGTGGTTC, (Reverse): ATACATACGGCTTCTCATTG; and ACTB (Forward): TGAAGATCAAGATCATTG, (Reverse): TAACGCAACTAAGTCATA.

Statistical analysis

The required sample size for the study was computed using parametric tests. We assumed that the variability of the expression levels obtained from the groups was 0.45 units. For repeated measurements, the variation of expression levels obtained over time from the samples was examined using the analysis of variance (ANOVA) method. A statistically significant difference was identified, and the sample size was determined as a significant difference with an effect size of 0.577 units at 90% power. It was resolved to include eight individuals in each experimental group for sample collection. This calculation was performed using G-Power (v. 3.0.10) software. Comparisons within dependent groups were conducted using the Paired t-test and the Repeated Measures ANOVA method. A p-value of less than 0.05 was deemed significant for statistical purposes. All statistical analyses and graphic preparations were performed using SPSS 21.0 for Windows.

The subject's privacy and confidentiality were assured, and the study received approval from the Hacettepe University Research Ethics Committee (#GO 18/573-04) on June 12, 2018. This research benefited from a grant provided by the Hacettepe University Research Foundation (Grant No: TSA-2018-17320) and was carried out in compliance with the Helsinki Declaration, as revised in 2013.

Ethics approval

Hacettepe University Research Ethics Committees (#GO 18/573-04) on 12 June 2018.

Consent to participate

All authors give consent to participation for this study.

Results

Cell poliferation assessment

The WST-1 test was applied to evaluate cell proliferation in the test groups and the HGL5. Cellular proliferation in the male factor and PCOS groups logarithmically exceeded 1 at the end of 24 h; however, there was no change in cellular proliferation after 48 h (Fig. 1). In the analysis performed with two-way ANOVA, there is a significant difference between the 24th, 48th and 72nd hours ($p < 0.05$). However, the 48th hour, when the first significant difference occurred in all three cell groups, was taken as a basis in the experiments.

Effective dose of FF-MAS in granulosa cells

The WST-1 viability test was utilized to determine the effective dose of FF-MAS in male factor, HGL5 cell line, and PCOS samples. Although there was no notable difference between 0.1 μM and 10 μM, a significant
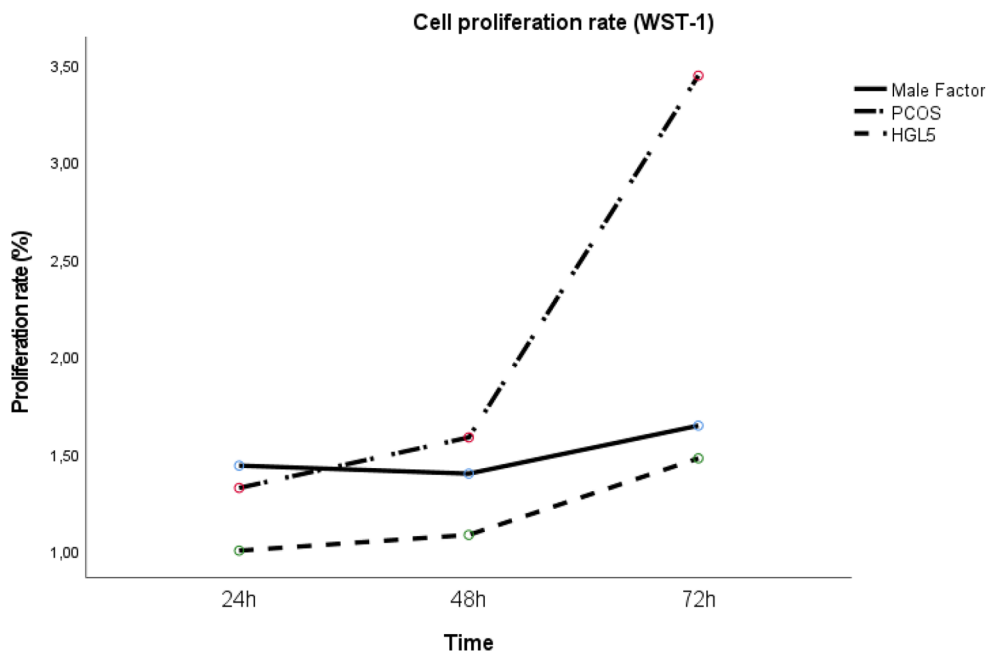

Figure 1. Cell proliferation rates of male factor, PCOS and HGL5 granulosa cells. Y axis indicates proliferation fold change number of cells.

discrepancy was observed between 10 μM and 100 μM of FF-MAS; we thus inferred that the highest non-toxic dose over 48 h was 10 μM (Fig. 2).

Immunohistochemistry results
Effect of FF-MAS
The Hedgehog (Hh) pathway components SMO and Gli1 were observed to be expressed in all granulosa cells of both male factor and PCOS groups. As the protein SMO is transmembranous, its expression was sighted on the cellular membrane (1st and 2nd rows in Fig. 3). The expression of SMO in the FF-MAS subgroups was statistically significantly higher than in the control subgroups ($p < 0.001$). This increase appeared more acute in the PCOS group than in the male factor group, however, the differences were not statistically significant (p: 0.078) between the male factor and PCOS groups (Part a in Fig. 4).

Gli1 expression was observed in both the nucleus and cytoplasm (3th and 4th rows in Fig. 3). Its expression was found to be higher in the FF-MAS group than in control subgroups, similar to the behavior observed in SMO expression (Part b in Fig. 4). When compared with the FF-MAS subgroup, Gli1 expression was significantly lower in the control subgroup ($p = 0.018$). Comparing FF-MAS subgroups, the response in the PCOS group was shown to be better than the MF group (PCOS FF-MAS group: 20.6365, Male Factor FF-MAS: 16.2419). The HGL5 cell line IF result confirmed these primary group results, used as a standardized control for both SMO and Gli1 (Figs. 5 and 6).

Effect of cyclopamine, only and with FF-MAS
SMO expression in the F + Cyc subgroup decreased significantly in comparison to the FF-MAS-only subgroup ($p < 0.001$). This decrease was particularly pronounced in the Cyc subgroup. Cyclopamine successfully suppressed both the pathway and SMO expression in both groups. Subgroups given F + Cyc exhibited lower expression than control subgroups. Yet, F + Cyc groups had higher IF expressions than the subgroups given only cyclopamine ($p < 0.05$) (Part a in Fig. 4).

When the Cyc subgroups of the PCOS and MF main groups were compared, Gli1 expression was more suppressed by cyclopamine in the PCOS group, but this difference was not significant ($p < 0.063$). In both of the main groups, cyclopamine subgroups had significantly lower expression than all other subgroups; however, the lowest was seen in the F + Cyc subgroups ($p < 0.001$). Gli1 expression in the F + Cyc subgroup was higher than in the cyclopamine subgroup ($p < 0.001$). In the HGL5 cell line, Gli1 expression was suppressed by cyclopamine, similarly to the patient samples. FF-MAS caused a significant increase in Gli1 expression in the F + Cyc subgroup despite the presence of cyclopamine, but the expression was still significantly lower compared to the control subgroups (Fig. 6).

Immunoperoxidase expressions were also consistent with immunofluorescence expressions (Supp Data Figs. 1, 2, 3 and 4). The data from the cytoELISA, a quantitative peroxidase-based method, were similar to other immunohistochemical results (Supp Data Fig. 5).

qRT-PCR
In the analysis of Gli1 transcription across all groups, gene expression was significantly increased by FF-MAS compared to all other subgroups ($p < 0.05$) (right of Fig. 7). While there was an increase in the PCOS group, SMO expression was significantly boosted by FF-MAS only within the male factor group (left of Fig. 7). Cyclopamine administration notably reduced SMO expression in both primary groups, while Gli1 expression essentially mirrored the control subgroup within the male factor group. For both SMO and Gli1, the F + Cyc subgroups displayed higher expression compared to the Cyc subgroup within the PCOS group alone; however, the results for the Cyc and F + Cyc subgroups were similar in the male factor group. In conclusion, FF-MAS elevated the mRNA levels of both proteins in samples from both the male factor and PCOS groups, but SMO elevation is not significant in PCOS group. On the other hand, cyclopamine significantly reduced the mRNA levels of both proteins only in the PCOS group.
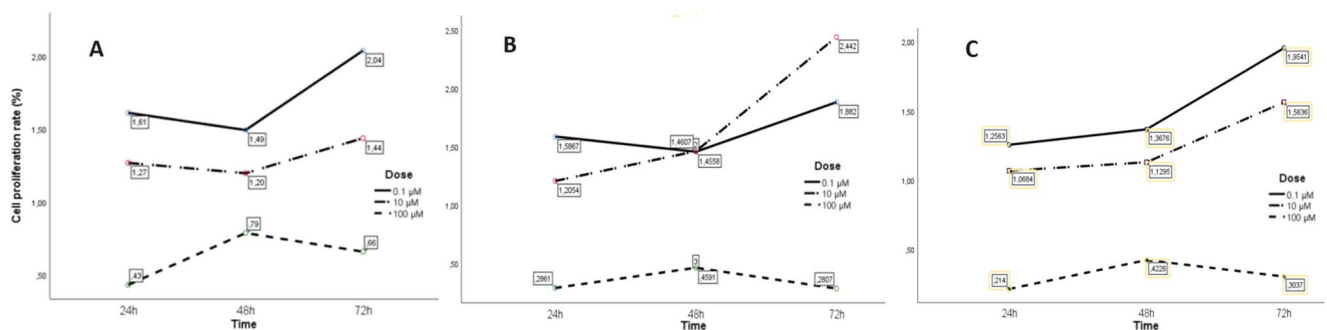

Figure 2. Cell proliferation rate (WST test) results of FF-MAS doses according to time. Figure A belongs to the male factor group, figure B to the PCOS group, and figure C to the HGL5 cell line. Since the interaction was 0.95 (> 0.05), no subgroup comparison was made. For all main groups, the effective dose and the shortest time in which proliferation first shows a significant increase is based on 48 h and 10μM FF-MAS dose were determined.
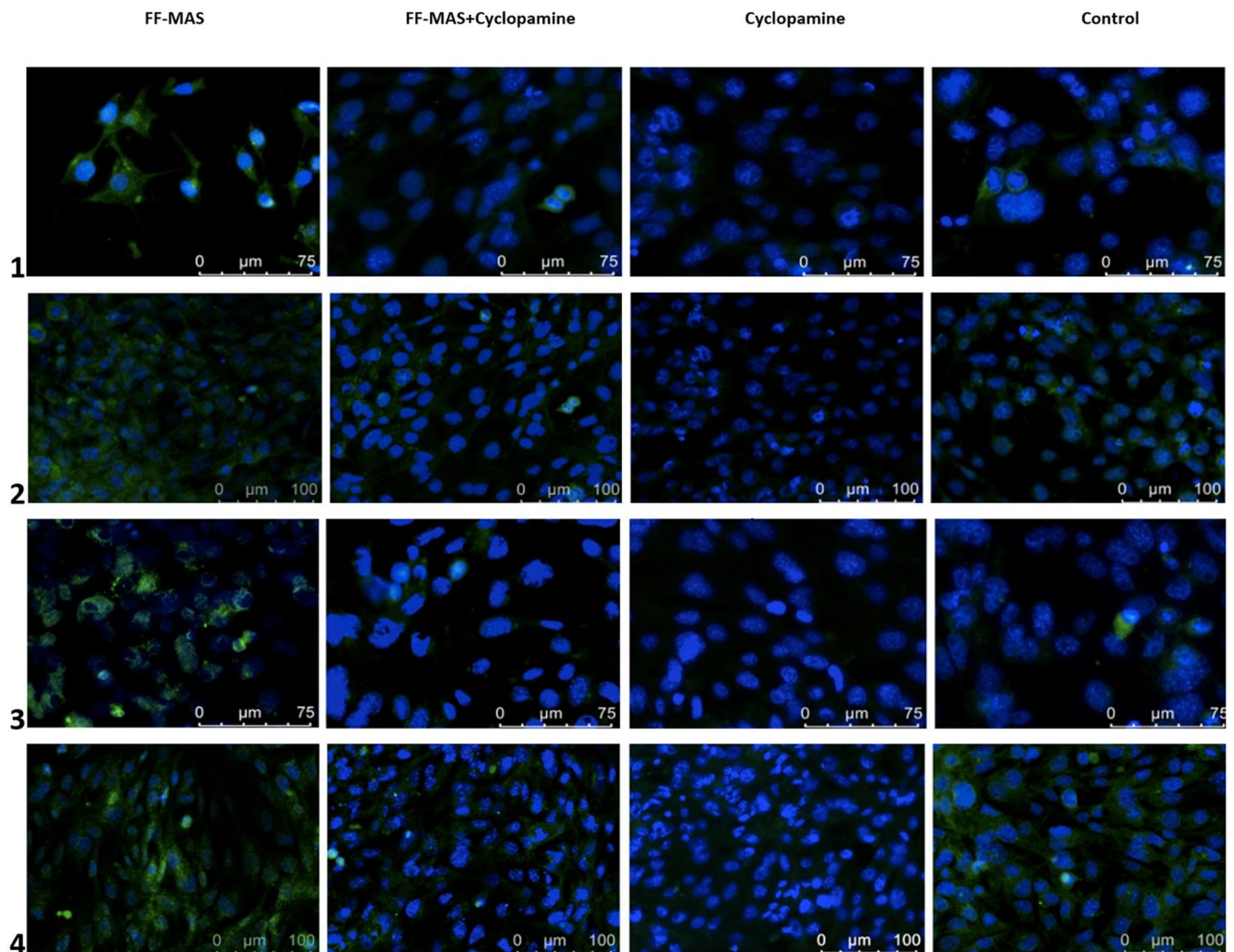
Figure 3. Immunoflourescence expressions of granulosa cells. 1st row: SMO in the male factor group, 2nd row: SMO in the PCOS group, 3th row: Gli1 in the male factor group, 4th row: Gli1 in the PCOS group (40x, green: SMO or Gli1, blue: DAPI).

Discussion

Steroidogenesis plays a significant role in cell physiology, being related to the functional activity and proliferation of various cells, such as adipocytes, hepatocytes, and myocytes. As such, disorders of steroidogenesis can influence many organs, with the ovary being particularly affected. The correlation between follicular development and steroidogenesis has been the focus of many recent studies on fertility[30,31]. PCOS, characterized by steroidogenesis failure and granulosa cell proliferation disorder, is a significant pathology in the female reproductive system as it can cause infertility.

Follicular fluid-meiosis activating sterol (FF-MAS) is an oxysterol obtained from follicular fluid and is demonstrated to exert a proliferative effect on folliculogenesis and embryogenesis[32]. It has been the topic of investigations regarding in vitro fertilization treatments[33,34]. Nonetheless, there is a lack of detailed cellular information concerning the molecular pathways that FF-MAS uses. In our study, we analyzed this effect through the components of the Hedgehog (Hh) pathway in granulosa cells from women in the male factor and PCOS groups. The standout aspect of our study was the impact of FF-MAS oxysterol in PCOS patients on granulosa cell proliferation and whether this effect is linked to the Hh pathway.

In our study, we first examined the possible relationship between the Hedgehog (Hh) pathway and FF-MAS based on the fact that the extracellular part of the Smoothened (SMO) receptor houses an oxysterol binding site[13,35]. The second reason was the role of cholesterol and its esters in the posttranscriptional modification of Hh ligands[36,37]. The connection between SMAD-1, SMAD-5, Notch, and phosphatidylinositol 3 kinase activation and cell proliferation in folliculogenesis is acknowledged, but the association of these pathways with cholesterol or its derivatives is not as apparent as with the Hh pathway. Given that the oxysterol-Hh pathway association has been established due to its role in steroidogenesis, we investigated whether FF-MAS, an oxysterol derivative, exerts its effect in the cell via the Hedgehog pathway in this study. Finally, we evaluated the relationship between
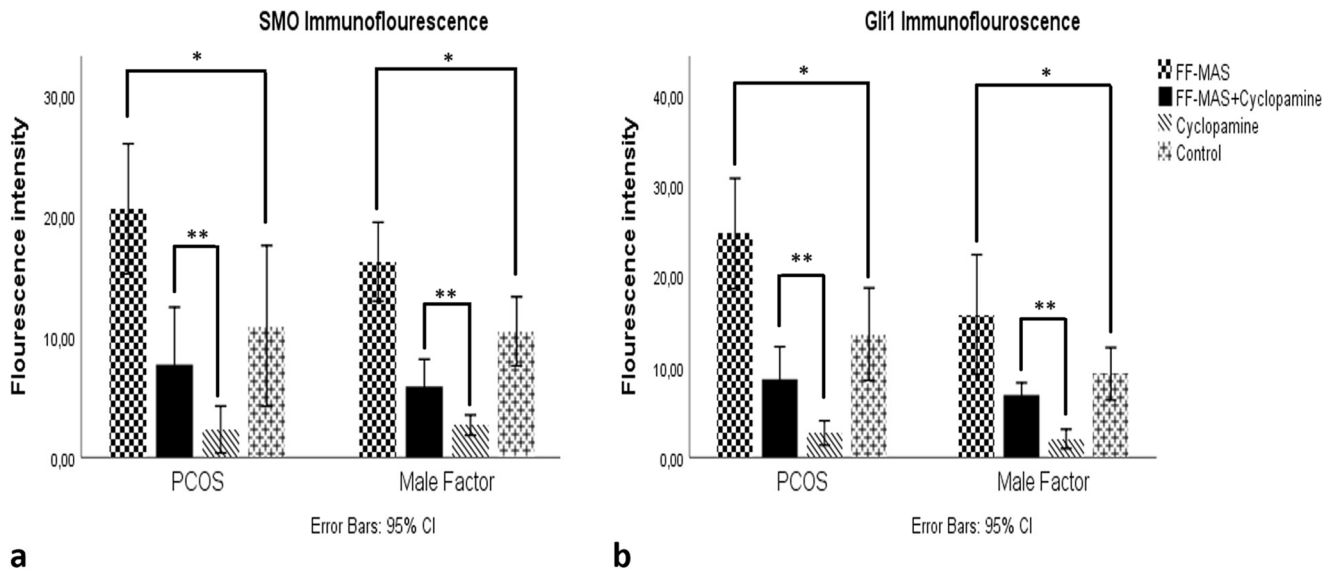
Figure 4. The data of immunoflourescence intensity in the male factor and PCOS groups: a: SMO, b: Gli1(* indicates $p < 0,01$, ** indicates $p < 0,05$).
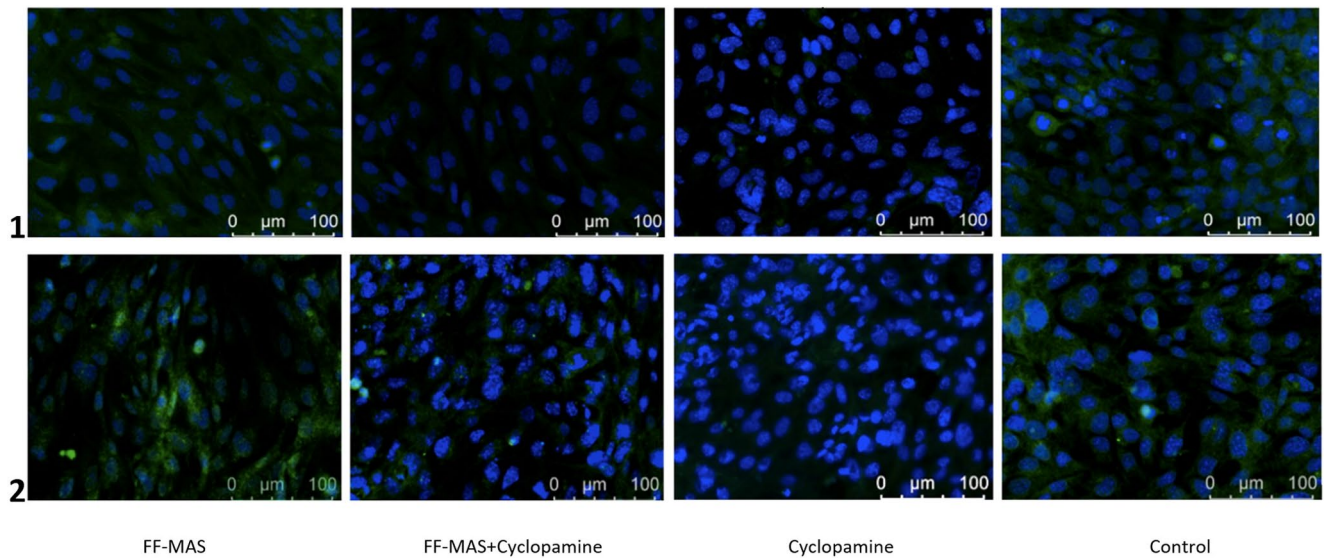

Figure 5. Immunofluorescence expressions of granulosa cells. 1st row: SMO in the HGL5 cells, 2nd row: Gli1 HGL5 cell line (40x, green: SMO or Gli1, blue: DAPI).

the Hh pathway and FF-MAS on the Smoothened (SMO) receptor and the resultant product of the Hh pathway, Gli1 protein.

Hh components, Ptch1 and Gli1, are co-expressed along with steroidogenic enzymes in both mouse and human adrenal cortex studies, and cortical hypoplasia has been observed in mutations of Ptch1 and Gli1 proteins[38,39]. It has also been reported that the Hh pathway's impact on granulosa and theca cells, where steroidogenesis plays a crucial role in hormone synthesis, influences cell proliferation and hormone synthesis[40,41]. The outcome of the cell proliferation experiments revealed that FF-MAS impacts granulosa cell proliferation in a dose-dependent manner. This research has contributed new information to the literature since it discusses the proliferation of granulosa cells – which play a significant role in various aspects of follicle growth – and thus the intracellular mechanisms of this effect of FF-MAS, which can influence the development of preantral-antral follicles.

As an alkaloid, cyclopamine is a selective inhibitor of the Hh pathway and exerts its inhibitory effect by binding to the pathway receptor, SMO[42]. In our study, the lowest expression was observed in all the immunofluorescence and immunoperoxidase results of the subgroups administered with only cyclopamine. By binding to SMO and inhibiting the pathway, cyclopamine targets existing SMOs, one of the Hh pathway components[43]. These components are in a continuously dynamic process of production and destruction, causing a decrease in
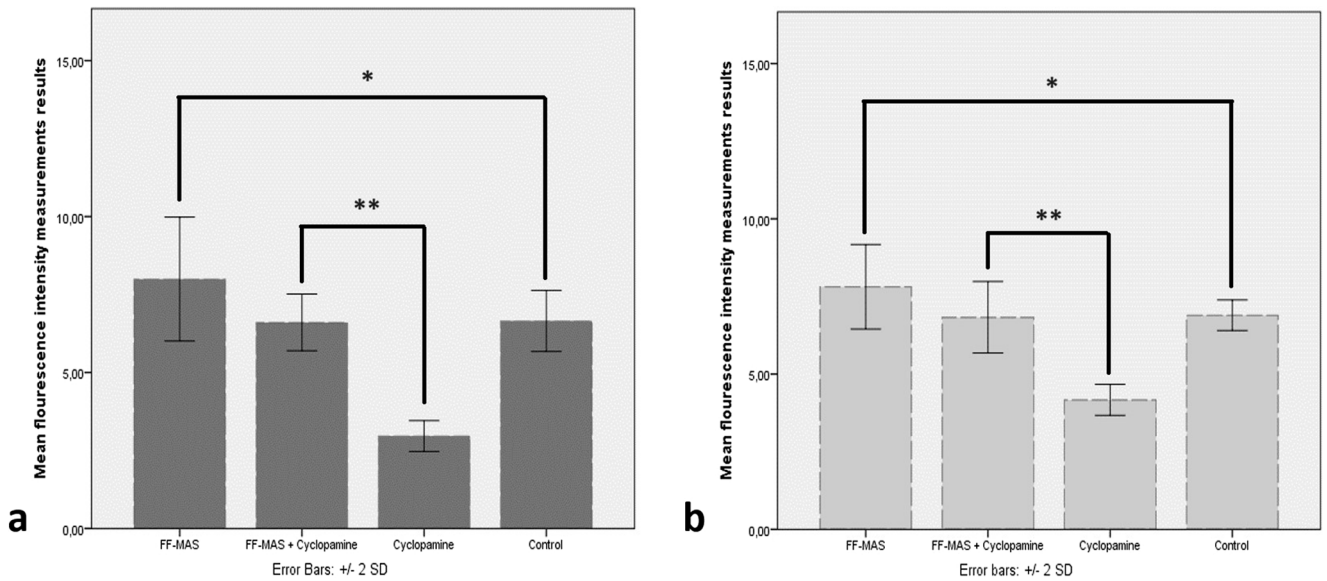
Figure 6. The data of immunoflourescence intensity in HGL5 cells: a: SMO, b: Gli1 (* indicates $p < 0,01$, ** indicates $p < 0,05$).
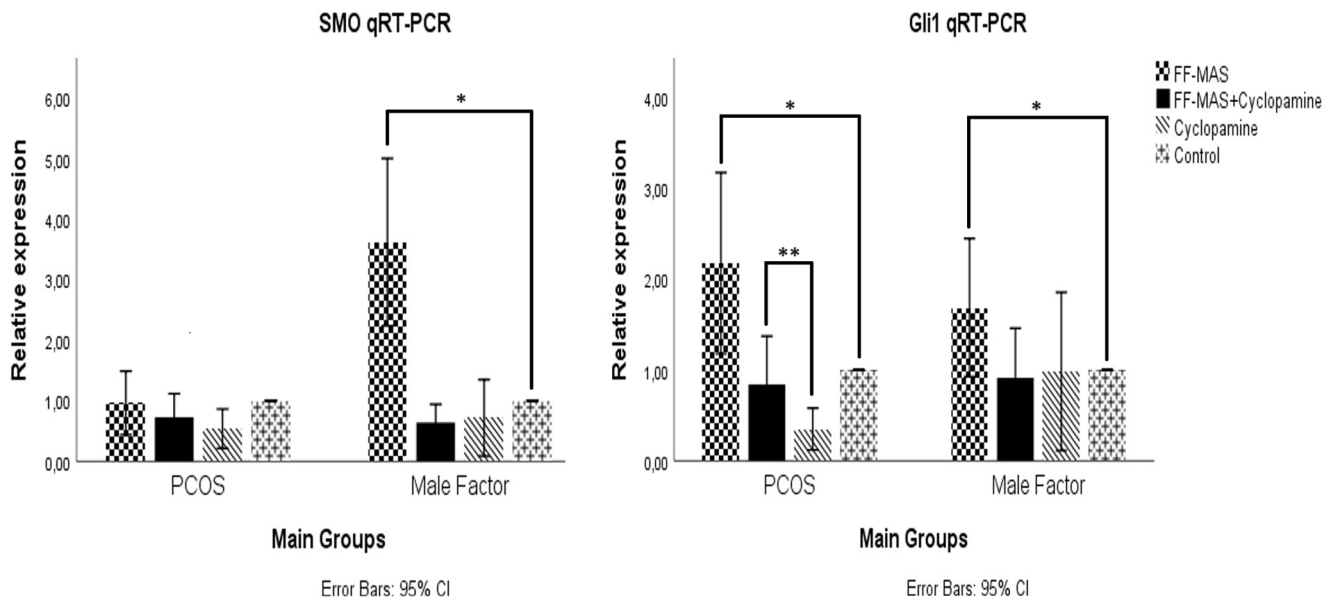

Figure 7. Quantitative real-time PCR results for left: SMO, right: Gli1 (* indicates $p < 0,01$, ** indicates $p < 0,05$).

expression by affecting the production of new SMOs. As such, even in low doses, our results revealed consistent expressions with the canonical pathway SMO and Gli1. These findings indicate that the experimental model used in this study was an effective method for achieving this goal. Considering the IF and IP results, when the Cyc subgroups of the PCOS and MF main groups were compared, it was seen that cyclopamine suppressed Gli1 expression more in the PCOS group, but this difference was not significant ($p < 0.063$). Our qRT-PCR results also support this finding. The possible reason for this is that while other pathways that increase Gli1 production are active in the MF group, these mechanisms may be impaired in PCOS patients. Repeating the study with a larger number of participants may make this result statistically significant.

In the F + Cyc groups, all immunofluorescent and immunoperoxidase expressions were consistent with each other. A significant decrease was observed in the expressions of both proteins compared to the F and CG subgroups. SMO and Gli1 expressions were suppressed by cyclopamine in the F + Cyc group, but they were higher than the Cyc subgroup. When qRT-PCR results were examined, the transcription levels of both proteins in MF groups were significantly increased by the administration of FF-MAS. In contrast, both gene expressions

increased in PCOS groups, while only Gli1 was statistically significantly increased. In the PCOS main group, the F + Cyc group showed higher results for both genes than the Cyc group, but only Gli1 was statistically significant. This suggests that the inductive effect of FF-MAS may occur via the Hh pathway, and this effect may persist despite cyclopamine inhibition. Similarly, Zou et al. reported that HDM/TGF-β1 stimulation resulted in higher Hh stimulation in human bronchial epithelial cells compared to the control, despite cyclopamine[44]. These results show that FF-MAS in granulosa cells mainly shows its effect via the canonical Hh pathway, but also increases Gli1 expression via other pathways etc. This suggests that both non-canonical Hh pathways and other cellular pathways that increase Gli1 expression can be assesed in future studies.

When comparing the CG subsets of granulosa cells in women with PCOS and those in the male factor groups, there was a marginally lower expression observed in the granulosa cells of the PCOS patients. However, this disparity was not statistically significant. These findings suggest that the Hh pathway demonstrates less activity in PCOS patients. This is further evidenced by the reduced proliferation in the control subgroups of PCOS, and lower SMO and Gli1 expressions, in comparison to the granulosa cells of the male factor group. This also indicates that the Hh pathway is less active in the PCOS group. Nevertheless, this conclusion can be contested and might be clarified with a larger sample size.

FF-MAS activity prompts an increase in both the SMO receptor protein and the Gli1 transcription factor via the canonical pathway of the Hh pathway, according to our hypothesis. We also observed this increase in the expression of Hh pathway components not only in the granulosa cells of the PCOS group but also in those of the male factor group. Consequently, the Hh signaling pathway or its interaction with FF-MAS may not be the primary cause of the pathogenesis of PCOS. Our findings suggest that future studies should consider the role of FF-MAS in the in vivo treatment of PCOS patients, especially since we noticed an increase in granulosa cell proliferation.

Data availability
The datasets generated and/or analyzed during the current study are not publicly available [as they contain volunteer participant data] but are available from the corresponding author upon reasonable request.

Code availability
There is no custom code or software application in our study.

References
1. Rotterdam, E. S. H. R. E. & ASRM-Sponsored PCOS consensus workshop group. Revised 2003 consensus on diagnostic criteria and long-term health risks related to polycystic ovary syndrome (PCOS). *Hum. Reprod.* **19** (1), 41–7. https://doi.org/10.1093/humrep/deh098 (2004).
2. Dewailly, D. et al. Definition and significance of polycystic ovarian morphology: a task force report from the Androgen Excess and Polycystic Ovary Syndrome Society.. *Hum. Reprod. Update* **20**(3), 334–352. https://doi.org/10.1093/humupd/dmt061 (2014).
3. Wojciech, P. & Ross, M. H. *Histology: A Text and Atlas: With Correlated Cell and Molecular Biology* 8th Edition. (2018). ISBN: 978-197-511-536-4
4. Turathum, B., Gao, E. M. & Chian, R. C. The function of Cumulus cells in Oocyte Growth and Maturation and in subsequent ovulation and fertilization. *Cells* **10**(9), 2292. https://doi.org/10.3390/cells10092292 (2021).
5. Wijgerde, M., Ooms, M., Hoogerbrugge, J. W. & Grootegoed, J. A. Hedgehog signaling in mouse ovary: Indian hedgehog and desert hedgehog from granulosa cells induce target gene expression in developing theca cells. *Endocrinology* **146**(8), 3558–3566. https://doi.org/10.1210/en.2005-0311 (2005).
6. Spicer, L. J. et al. The hedgehog-patched signaling pathway and function in the mammalian ovary: a novel role for hedgehog proteins in stimulating proliferation and steroidogenesis of theca cells. *Reproduction* **138** (2), 329–39. https://doi.org/10.1530/REP-08-0317 (2009).
7. Nguyen, N. T. et al. Sonic hedgehog promotes porcine oocyte maturation and early embryo development. *Reprod. Fertil. Dev.* **21** (6), 805–15. https://doi.org/10.1071/RD08277 (2009).
8. Liu, C., Peng, J., Matzuk, M. M. & Yao, H. H. Lineage specification of ovarian theca cells requires multicellular interactions via oocyte and granulosa cells. *Nat. Commun.* **6**, 6934. https://doi.org/10.1038/ncomms7934 (2015).
9. Nguyen, N. T., Lo, N. W., Chuang, S. P., Jian, Y. L. & Ju, J. C. Sonic hedgehog supplementation of oocyte and embryo culture media enhances development of IVF porcine embryos. *Reproduction* **142**(1), 87–97. https://doi.org/10.1530/REP-11-0049 (2011).
10. Carballo, G. B., Honorato, J. R., de Lopes, G. P. F. & Spohr, T. C. L. S. E. A highlight on sonic hedgehog pathway. *Cell. Commun. Signal.* **16**(1), 11. https://doi.org/10.1186/s12964-018-0220-7 (2018).
11. Robbins, D. J., Fei, D. L. & Riobo, N. A. The hedgehog signal transduction network. *Sci. Signal.* **5**(246), re6. https://doi.org/10.1126/scisignal.2002906 (2012).
12. Lee, S. T. et al. Cyclopamine: from cyclops lambs to cancer treatment. *J. Agric. Food Chem.* **62**(30), 7355–7362. https://doi.org/10.1021/jf5005622 (2014).
13. Griffiths, W. J. et al. Current trends in oxysterol research. *Biochem. Soc. Trans.* **44**(2), 652–658. https://doi.org/10.1042/BST20150255 (2016).
14. Griffiths, W. J. & Wang, Y. Oxysterol research: a brief review. *Biochem. Soc. Trans.* **47**(2), 517–526. https://doi.org/10.1042/BST20180135 (2019).
15. Byskov, A. G., Baltsen, M. & Andersen, C. Y. Meiosis-activating sterols: background, discovery, and possible use. *J. Mol. Med. (Berl)* **76** (12), 818–23. https://doi.org/10.1007/s001090050286 (1998).
16. Jamnongjit, M. & Hammes, S. R. Oocyte maturation: the coming of age of a germ cell. *Semin Reprod. Med.* **23**(3), 234–241. https://doi.org/10.1055/s-2005-872451 (2005).
17. Byskov, A. G., Andersen, C. Y. & Leonardsen, L. Role of meiosis activating sterols, MAS, in induced oocyte maturation. *Mol. Cell Endocrinol.* **187** (1–2), 189–96. https://doi.org/10.1016/s0303-7207(01)00707-9. (2002).
18. Marín Bivens, C. L. et al. A synthetic analogue of meiosis-activating sterol (FF-MAS) is a potent agonist promoting meiotic maturation and preimplantation development of mouse oocytes maturing in vitro. *Hum. Reprod.* **19**(10), 2340–2344. https://doi.org/10.1093/humrep/deh436 (2004).

19. Guo, R. et al. Follicular fluid meiosis-activating sterol (FF-MAS) promotes meiotic resumption via the MAPK pathway in porcine oocytes. *Theriogenology* **148**, 186–193 (2020).
20. Dilower, I. et al. Hedgehog signaling in gonadal development and function. *Cells* **12**(3), 358. https://doi.org/10.3390/cells12030358 (2023).
21. Tsai, Y. R., Liao, Y. N. & Kang, H. Y. Current advances in Cellular approaches for Pathophysiology and Treatment of Polycystic Ovary Syndrome. *Cells* **12**(17), 2189. https://doi.org/10.3390/cells12172189 (2023).
22. Arensdorf, A. M., Marada, S., Ogden, S. K. & Smoothened Regulation,. A tale of two signals. *Trends Pharmacol. Sci.* **37**(1), 62–72. https://doi.org/10.1016/j.tips.2015.09.001 (2016).
23. Huang, P. et al. Cellular cholesterol directly activates smoothened in hedgehog signaling. *Cell* **166**(5), 1176-1187e14. https://doi.org/10.1016/j.cell.2016.08.003 (2016).
24. Zırh, S. et al. A new isolation and culture method for granulosa cells. *Cell. Tissue Bank.* **22**(4), 719–726. https://doi.org/10.1007/s10561-021-09929-5 (2021).
25. van der Horst, G., Farih-Sips, H., Löwik, C. W. & Karperien, M. Hedgehog stimulates only osteoblastic differentiation of undifferentiated KS483 cells. *Bone* **33** (6), 899–910. https://doi.org/10.1016/j.bone.2003.07.004 (2003).
26. Yu, Y. et al. Overexpression of Gremlin 1 by sonic hedgehog signaling promotes pancreatic cancer progression. *Int. J. Oncol.* **53**(6), 2445–2457. https://doi.org/10.3892/ijo.2018.4573 (2018).
27. Tan, W. J. et al. MED12 protein expression in breast fibroepithelial lesions: correlation with mutation status and oestrogen receptor expression. *J. Clin. Pathol.* **69**(10), 858–865. https://doi.org/10.1136/jclinpath-2015-203590 (2016).
28. Jensen, E. C. Quantitative analysis of histological staining and fluorescence using ImageJ. *Anat. Rec. (Hoboken)* **296** (3), 378–81.https://doi.org/10.1002/ar.22641. (2013).
29. Livak, K. J & Schmittgen, T. D. Analysis of relative gene expression data using real-time quantitative PCR and the 2(-Delta Delta C(T)) Method. *Methods* **25** (4), 402-8. https://doi.org/10.1006/meth.2001.1262. (2001).
30. Azziz, R. Polycystic Ovary Syndrome. *Obstet. Gynecol.* **132** (2), 321–336. https://doi.org/10.1097/AOG.0000000000002698. (2018).
31. Spitschak, M. & Hoeflich, A. Potential functions of IGFBP-2 for ovarian folliculogenesis and Steroidogenesis. *Front. Endocrinol. (Lausanne)* **9**, 119. https://doi.org/10.3389/fendo.2018.00119 (2018).
32. Fakheri, R. J. & Javitt, N. B. Autoregulation of cholesterol synthesis: physiologic and pathophysiologic consequences. *Steroids* **76**(3), 211–215. https://doi.org/10.1016/j.steroids.2010.10.003 (2011).
33. Hao, R., Zhang, C., Lv, L., Shi, L. & Yue, W. Effects of AY9944 A-7 on gonadotropin-induced meiotic resumption of oocytes and development of parthenogenetic embryos in sheep. *Theriogenology* **83**(1), 30–37. https://doi.org/10.1016/j.theriogenology.2014.06.025 (2015).
34. Marco-Jiménez, F., Llobat, L. & Vicente, J. S. Effects of lanosterol on in vitro maturation of porcine oocytes. *Anim. Reprod. Sci.* **117**(3–4), 288–294. https://doi.org/10.1016/j.anireprosci.2009.04.008 (2010).
35. Brown, A.J & Sharpe, L.J. Oxysterols. In: Offermanns, S., Rosenthal, W. (eds) *Encyclopedia of Molecular Pharmacology.* (Springer, Cham, 2021). https://doi.org/10.1007/978-3-030-57401-7_10016.
36. Blanc, M. et al. The transcription factor STAT-1 couples macrophage synthesis of 25-hydroxycholesterol to the interferon antiviral response. *Immunity* **38**(1), 106–118. https://doi.org/10.1016/j.immuni.2012.11.004 (2013).
37. Jeong, J. & McMahon, A. P. Cholesterol modification of hedgehog family proteins. *J. Clin. Invest.* **110**(5), 591–596. https://doi.org/10.1172/JCI16506 (2002).
38. Huang, C. C., Miyagawa, S., Matsumaru, D., Parker, K. L. & Yao, H. H. Progenitor cell expansion and organ size of mouse adrenal is regulated by sonic hedgehog. *Endocrinology* **151**(3), 1119–1128. https://doi.org/10.1210/en.2009-0814 (2010).
39. King, P., Paul, A. & Laufer, E. Shh signaling regulates adrenocortical development and identifies progenitors of steroidogenic lineages. *Proc. Natl. Acad. Sci. U S A* **106**(50), 21185–21190. https://doi.org/10.1073/pnas.0909471106 (2009).
40. Finco, I., LaPensee, C. R., Krill, K. T. & Hammer, G. D. Hedgehog signaling and steroidogenesis. *Annu. Rev. Physiol.* **77**, 105–129. https://doi.org/10.1146/annurev-physiol-061214-111754 (2015).
41. Miller, W. L. & Bose, H. S. Early steps in steroidogenesis: intracellular cholesterol trafficking. *J. Lipid Res.* **52**(12), 2111–2135. https://doi.org/10.1194/jlr.R016675 (2011).
42. Galperin, I., Dempwolff, L., Diederich, W. E. & Lauth, M. Inhibiting hedgehog: an update on pharmacological compounds and targeting strategies. *J. Med. Chem.* **62**(18), 8392–8411. https://doi.org/10.1021/acs.jmedchem.9b00188 (2019).
43. Torroja, C., Gorfinkiel, N. & Guerrero, I. Mechanisms of Hedgehog gradient formation and interpretation. *J. Neurobiol.* **64** (4), 334–56. https://doi.org/10.1002/neu.20168. (2005).
44. Zou, Y., Song, W., Zhou, L., Mao, Y. & Hong, W. House dust mite induces sonic hedgehog signaling that mediates epithelial–mesenchymal transition in human bronchial epithelial cells. *Mol. Med. Rep.* **20**(5), 4674–4682. https://doi.org/10.3892/mmr.2019.10707 (2019).

Author contributions

Declarations

Competing interests

The authors declare no competing interests.

Grant

Consent for publication

All authors give consent for publication for this study.

Additional information